第1卷 第2期
1 9 8 6年10月

航空动力学报
Journal of Aerospace Power

Vol.1 No.2
Oct. 1986

有裂纹悬臂转子的振动特性

西北工业大学 顾家柳 王能谦

摘 要

本文研究了轴具有横向裂纹的高速悬臂转子的振动特性，提出了监视此裂纹起始及发展的最佳方法。所研究的模型是按一航空涡轮转子建立的，理论分析借传递矩阵-直接积分法[1,2]，即借传递矩阵导出运动方程，再借直接积分法求解。还对模型裂纹转子作了试验研究，试验结果与理论计算结果在性质上是一致的。通过这一研究发现，转子不平衡响应的三次谐波可能是监视这一类型转子裂纹起始与发展的首要频率分量。

一、引 言

近年内，曾发生过因涡轮轴裂纹扩展致使轴折断，造成严重后果的事故。为了保证飞行的安全，可以借振动监视裂纹的起始与发展。因此，首先必须了解带有裂纹轴转子的振动特性。本文从理论上和实验上研究带有裂纹轴的高速悬臂转子的振动特性。

与其它研究〔3～6〕的不同之处是：本文在理论分析中采用了传递矩阵-直接积分法〔1,2〕，对转子的进动轨迹不作任何假设；借一定技术使制造出的裂纹十分接近于真实的裂纹。

二、涡轮转子的简化模型

本文所分析的涡轮转子简化模型如图1所示。图中$m = 5kg$，$J_p = 2J_d = 300kg\text{-}cm^2$，$l_1 = 15cm$，$l_2 = 56cm$，$c_1 = c_2 = 6～20\times10^4 N/cm$ （3组），$J_1 = 1.92cm^4$，$J_2 = J_3 = 3.97cm^4$，$D_1 = 2.5cm$，$D_2 = D_3 = 3cm$。

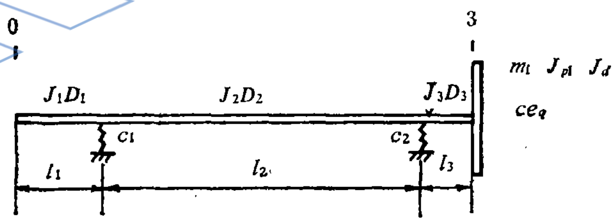

图1 模型转子

转子的前端为一柔性联轴节，盘具有力不衡度Ge，转子支于两个弹性支承上，裂纹位于悬臂段。借共振放大因子来估计等效阻尼系数c_{eq}，对于航空燃气涡轮发动机，共振放大因子约为10～20。

三、运 动 方 程

采用四种坐标系：固定坐标系OXYZ，旋转坐标系OX′Y′Z′(旋转速度同转子的旋转速度ω)和$O\xi\eta S$(旋转速度等于转子的进动速度)，及固定于盘上的动坐标系O′X″Y″Z″(图2)。

用挠度x、y及挠角α、β作为转子的广义坐标。假定当t等于0时，裂纹刚好垂直于x轴，而不平衡量的初相位为i。

本文于1986年1月收到。

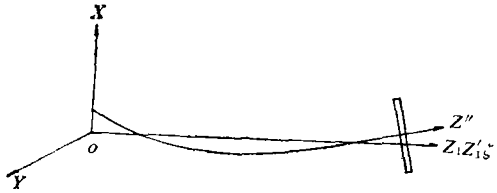

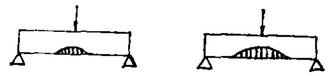

图 3　裂纹影响区

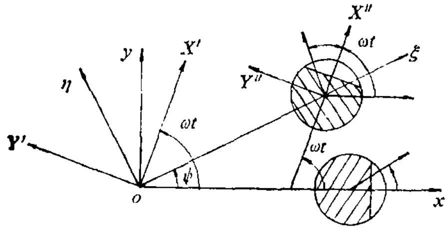

图 2　坐标系及初相位

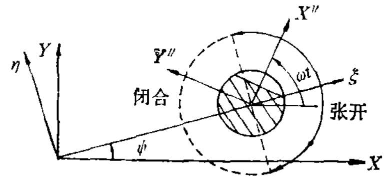

图 4　裂纹的开与合

根据裂纹的深浅不同，因裂纹而使轴刚度减小的影响范围也不同，如图 3 所示。本文中假定，在此影响段内，刚度减小是均匀的。当转子作一般进动时，裂纹交替地时开时合，如图 4 所示。可以根据裂纹的瞬时位置来判断其开合，当裂纹张开时，局部刚度（影响段内的 $J_{y''}$减小）；当裂纹闭合时，刚度保持不变。

基于上述模型及假设，可以用传递矩阵-直接积分法导出特征盘的运动方程并求解。由于借此方法导出运动方程及求解的过程在文献〔1、2〕中已经详述，故本文就不再赘述。唯一要说明的是，由于裂纹的开合作用，影响段传递矩阵的元素是时变的，因此运动方程首先在动坐标系ox′y′z′内导出，然后借坐标转换得到在固定坐标系内的运动方程：

$$\left.\begin{aligned}
&\frac{d^2x}{d\tau^2}+\frac{Ceq_1}{m\omega}\frac{dx}{d\tau}+(AA1\cos^2\tau+BB1\sin^2\tau)\frac{1}{m\omega^2}x+(AA1-BB1)\cdot\frac{\sin\tau\cos\tau}{m\omega^2}y\\
&\quad+(AA2-BB2)\frac{\sin\tau\cos\tau}{m\omega^2}\cdot\alpha+(AA2\cos^2\tau+BB2\sin^2\tau)\frac{1}{m\omega^2}\beta=e\cdot\cos(\tau+i)\\
&\frac{d^2y}{d\tau^2}+\frac{Ceq_1}{m\omega}\frac{dy}{d\tau}+(AA1\sin^2\tau+BB1\cos^2\tau)\frac{1}{m\omega^2}Y+(AA1-BB1)\frac{\sin\tau\cos\tau}{m\omega^2}x\\
&\quad+(AA2\sin^2\tau+BB2\cos^2\tau)\frac{1}{m\omega^2}\alpha+(AA2-BB2)\frac{\sin\tau\cos\tau}{m\omega^2}\beta=e\cdot\sin(\tau+i)-\frac{g}{\omega^2}\\
&\frac{d^2\alpha}{d\tau^2}+\frac{Ceq_2}{J_d\omega}\frac{d\alpha}{d\tau}+(AA3\sin^2\tau+BB3\cos^2\tau)\frac{1}{J_d\omega^2}\alpha-2\frac{d\beta}{d\tau}+(AA3-BB3)\frac{\sin\tau\cos\tau}{J_d\omega^2}\beta\\
&\quad-(AA4-BB4)\frac{\sin\tau\cos\tau}{J_d\omega^2}x-(AA4\sin^2\tau+BB4\cos\tau)\frac{1}{J_d\omega^2}y=0\\
&\frac{d^2\beta}{d\tau^2}+\frac{Ceq_2}{J_d\omega}\frac{d\beta}{d\tau}+(AA3\cos^2\tau+BB3\sin^2\tau)\frac{1}{J_d\omega^2}\beta+2\frac{d\alpha}{d\tau}+(AA3-BB3)\frac{\sin\tau\cos\tau}{J_d\omega^2}\alpha\\
&\quad-(AA_4\cos^2\tau+BB4\sin^2\tau)\frac{1}{J_d\omega^2}x-(AA4-BB4)\frac{\sin\tau\cos\tau}{J_d\omega^2}Y=0
\end{aligned}\right\}\quad(1)$$

式中

$\tau=\omega t$

$$\begin{aligned}
&AA1=\frac{a_{31}a_{43}-a_{33}a_{41}}{a_{33}a_{44}-a_{34}a_{43}} &&BB1=\frac{b_{31}b_{43}-b_{33}b_{41}}{b_{33}b_{44}-b_{34}b_{43}}\\
&AA2=\frac{a_{32}a_{43}-a_{33}a_{42}}{a_{33}a_{44}-a_{34}a_{43}} &&BB2=\frac{b_{32}b_{43}-b_{33}b_{42}}{b_{33}b_{44}-b_{34}b_{43}}\\
&AA3=\frac{a_{34}a_{42}-a_{32}a_{44}}{a_{33}a_{44}-a_{34}a_{43}} &&BB3=\frac{b_{34}b_{42}-b_{32}b_{44}}{b_{33}b_{44}-b_{34}b_{43}}\\
&AA4=\frac{a_{31}a_{44}-a_{34}a_{41}}{a_{33}a_{44}-a_{34}a_{43}} &&BB4=\frac{b_{31}b_{44}-b_{34}b_{41}}{b_{33}b_{44}-b_{34}b_{43}}
\end{aligned}\quad(2)$$

其中$a_{11}\cdots\cdots a_{44}$，$b_{11}\cdots\cdots b_{44}$相应为动坐标系内从o截面到 3 截面的总传递矩阵〔$A^{x'}$〕、〔$A^{y'}$〕的元素。这里注角x'，y'代表分别属于$x'oz'$、$y'oz'$平面。m、J_p、J_d分别为盘的质量、极和直径惯性矩，g为重力加速度。

四、运动方程的求解及结果

为便于比较，计算中除了偏心距e(取为0.002cm)、裂纹深度、影响区长度以外，其它结构参数均取自试验的模型转子系统(参见图 1)。方程(1)用数值积分法求解，再对解得的x作付里叶分析。为了使积分的初值尽可能准确，取运动方程简化为线性方程后的理论解，作为数值积分的初值。计算的部分结果如下面的表中所示。

表 1　转速改变时响应中各阶分量的变化(cm)

	$J_x'/J_y'=0.875$,			$i=0.314$ rad	
转速(1/s)	75	150	225	300	375
基频成分	0.507×10^{-6}	0.103×10^{-5}	0.944×10^{-6}	0.423×10^{-5}	0.243×10^{-4}
二阶分量	0.205×10^{-4}	0.166×10^{-3}	0.464×10^{-3}	0.103×10^{-2}	0.206×10^{-2}
三阶分量	0.479×10^{-4}	0.630×10^{-4}	0.906×10^{-4}	0.405×10^{-4}	0.520×10^{-4}
四阶分量	0.224×10^{-4}	0.419×10^{-4}	0.175×10^{-4}	0.951×10^{-5}	0.172×10^{-4}
五阶分量	0.683×10^{-5}	0.115×10^{-5}	0.152×10^{-5}	0.356×10^{-5}	0.579×10^{-5}
ω/ω_{cr}	1/6	1/3	1/2	2/3	5/6

表 2　裂纹深度不同时各阶分量的变化(cm)

		$\omega=150$rad/s,		$i=0.314$rad	
J_x'/J_y'	0.950	0.900	0.875	0.850	0.800
基频成分	0.101×10^{-5}	0.999×10^{-6}	0.103×10^{-5}	0.993×10^{-6}	0.994×10^{-6}
二阶分量	0.137×10^{-3}	0.139×10^{-3}	0.166×10^{-3}	0.141×10^{-3}	0.143×10^{-3}
三阶分量	0.549×10^{-4}	0.580×10^{-4}	0.630×10^{-4}	0.616×10^{-4}	0.656×10^{-4}
四阶分量	0.444×10^{-4}	0.419×10^{-4}	0.419×10^{-4}	0.391×10^{-4}	0.360×10^{-4}
五阶分量	0.131×10^{-5}	0.124×10^{-5}	0.115×10^{-5}	0.116×10^{-5}	0.107×10^{-5}

从计算结果可见，当轴裂纹时，转子的不平衡响应中不仅含有很强的二阶分量，而且还含有相当强的三阶分量，并且随着裂纹的扩展而增大(见表 2)。三阶分量还随转速而变，在$\omega/\omega_{cr}=1/3\sim1/2$时达到最大。

五、试　验　研　究

试验设备及测量仪器配置的示意图如图 5 所示。

试验结果表明，裂纹转子（试验件之裂纹深度为8.2毫米，相应于$J_{x'}/J_{y'}=0.574$)的不平衡响应中含有很强的三阶分量。这一分量随着转速的上升而增大，当转速增大到等于 1/3 临界转速(ω_{cr})时达最大值。转速继续上升，三阶分量逐渐减小，当转速超过ω_{cr}后，变得越来越小。而无裂纹转子的不平衡响应中，就不存在三次谐波。

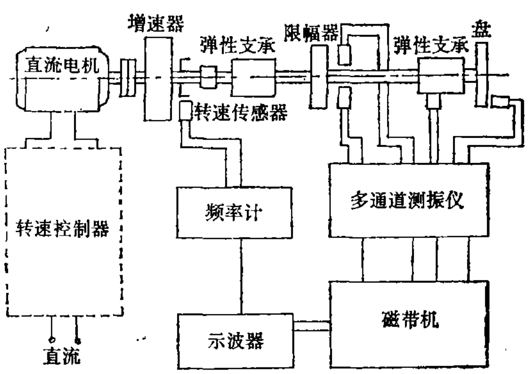

图 5　试验设备及测量系统框图

图 6 、7 所示分别为无裂纹及有裂纹的转子在$\omega=1/3$临界转速时的振动功率谱。图 6 所示无裂纹转子振动功率谱中的二阶分量，可能是联轴器不对中等因素所引起。

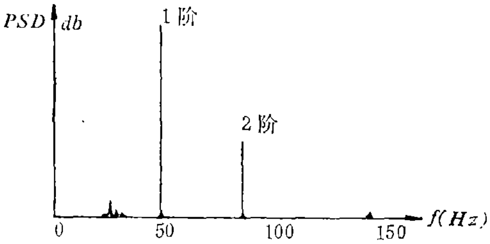

图 6　无裂纹转子试验的振动功率谱($\omega/\omega_{cr}=1/3$)

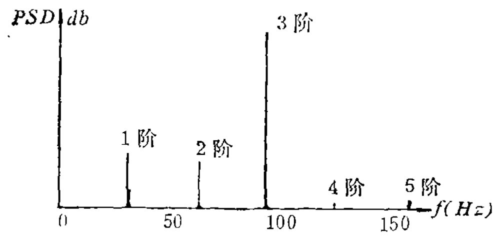

图 7　有裂纹转子试验的振动功率谱($\omega/\omega_{cr}=1/3$)

六、结　束　语

将试验结果与理论分析结果（图6、7与表1、2）相比较可见，二者在性质上是一致的。当裂纹转子在亚临界状态下运行时，振动谱中含有相当强的三次谐波。它随转速的上升而增大，到转速约等于1/3临界转速时达到极大值。当转子在超临界状态下运行时，这一个 三 阶分量近乎消失。

基于这一研究，作者认为：因为由裂纹的起始与发展所引起的基频及二阶分量的变化，可能被平衡破坏、对中度恶化等因素引起的基频及二阶分量的变化所混淆，将转子运行于转速等于1/3临界转速附近，并检测其振动响应中的三阶分量，可能是最有效的裂纹振动 监 视方法。当然还有待在实际机械中实践证实。

计算结果中的误差，可能来自以下几个方面：在计算中将弹性支承简化为一个静刚度；对裂纹影响段的假设与实际有差异；未考虑联轴器不对中等实际因素的影响；所取的不平衡度、裂纹深度与实际试验者不同；等等。

最后，作者在此谨向在试验中曾给过宝贵帮助的刘启洲、刘德馨二位同志表示谢意。

参 考 文 献

〔1〕 顾家柳，"传递矩阵——直接积分法及其应用，"航空学报第 4 卷第 4 期，1983

〔2〕 Gu Jialiu,"An Improved Transfer Matrix-Direct Integration Method for Rotor Dynamics,"10th Biennial Conference on Mechanical Vibration and Noise of The ASME,Cincinnati, USA, Sept. 10—13,1985,ASME Paper No.85-DET-27.

〔3〕 Henry,T.A.and Okah-Avae,B.E.,"Vibrations in Cracked Shafts",I.Mech.E. Conference Publications 1976—9,pp.15—20.

〔4〕 Mayes,I.W. and Davies,W.G.R.,"The Vibrational Behaviour of a Rotating Shaft System Containing a Transverse Crack",I Mech E Conference Publications 1976—9 ,pp.53—64.

〔5〕 Mayes,I.W.and Davies,W.G.R.,"A Method of Calculating the Vibrational Behaviour of Coupled Rotating Shafts Containing a Transverse Crack,"I Mech E Publivations 1980—4, pp.17—28.

〔6〕 Gasch,R., "Dynamic Behaviour of a Simple Rotor with a Cross-Sectional Crack",I. Mech. E. Conference Publications 1976—9,pp.123—126.

（责任编辑　李其汉）

A METHOD FOR CALCULATION OF FLOW PROCESS IN AN AXISYMMETRIC STRAIGHT-WALL ANNULAR DIFFUSER

Hua Guangshi

(*Northwestern Polytechnical University*)

Abstract

A complete method for calculation of the steady compressible flow in an axisymmetric atraight-wall annular diffuser with boundary layer correction based on streamtube method has been developed. One of the main features is that,for determination of the static pressure(p_{i+1}) at any downstream section from the inlet, two correlated formulas for direct and accurate calculation of the values of λ_{i+1} and p_{i+1} respectively are derived.Therefore, the iterative process as used in reference (1) might be avoided and the CPU time is then greatly reduced if the new solution procedure of the present study is employed.

Calculations have been carried out for a short annular diffuser . The results are all in very good agreement with experimental data. The calculations show that, if $\alpha_U=\alpha_L=\alpha$ (half the diffuser wall angle) and both wall friction and divergence losses are taken into account, $\alpha<8°$ and diffuser area ratio less than 1.46 are recommendable. This method is also applicable to the calculation of flow fields in a pre-diffuser of a short annular combustor-dump diffuser or in a two-dimensional straight-wall diffuser.

VIBRATIONAL CHARACTERISTICS OF THE CANTILEVER ROTOR WITH A CRACKED SHAFT

Gu Jialiu and Wang Nengqan

(*Northwestern Polytechnical University*)

Abstract

The vibrational characteristics of the high speed cantilever rotor with a cracked shaft are investigated to find an optimum vibration monitoring method for a turbine rotor. The model studied is established based on the structure of a real turbine rotor.

The transfer matrix-direct integration method proposed by the first author in reference (2) is applied to the theoretical analysis. In consequence it is possible

to avoid making any assumption about the whirling orbit, and modification of some real parameters and whirling orbit of the disk is performed sequentially in the process of numerical integration. In experimental investigation some measures are taken to create a crack very similar to a real crack on the shaft.

The results of Fourier analysis of the unbalance responses obtained from both calculations and experiments show that in signature of vibration of the cracked rotor exist very strong 2nd anc 3rd harmonics. The triple-frequency harmonic increases with the rotating speed and reaches maximum at the speed being equal to 1/3 of the critical speed.

Since the second harmonic can be caused by the other factors such as misalignment, as a result of this research the authors suggest that operating the rotor in the vicinity of 1/3 of the critical speed and monitoring the triple-frequency component be the best method to detect a crack for this kind of turbine.

EFFECTS OF THREE CENTRES OF BLADE ON FLUTTERING

Zhang Chengsheng and Song Zhaohong

(Beijing Institute of Aeronautics and Astronautics)

Abstract

The effects of three centres, i.e. aerodynamic centre, centre of gravity and centre of torsion, of blade on fluttering have been studied. A structural model of the coupling between bending and torsion is presented in the theoretical analysis. According to their dependence of the displacements of the blade vibration, the aerodynamic loads are considered as a function of the velocities of the blade vibration. The complex eigenvalue equations are resolved by iteration approach.

The conclusions drawn from the study are as follows: the blade with the forward centre of torsion is less stable than the blade with the backward one; the blade with the forward centre of gravity is more stable than the blade with the backward one. In the case of the blade with the foreward torsion centre, its stability is improved when the aerodynamic centre takes place between the gravity centre and the torsion centre. As far as the blade with backward torsion centre is concerned, the blade will be unstable when the aerodynamic centre is located between the gravity centre and the torsion centre. The analysis of these three different kinds of blades demonstrates that the blade with the aerodynamic centre located at the leading edge of the blade is the best one.